Search for supersymmetry in the multijet and missing transverse momentum final state: an analysis performed on 2.3 fb^{-1} of 13 TeV pp collision data collected with the CMS detector

John Bradmiller-Feld, on behalf of the CMS Collaboration
Department of Physics, University of California, Santa Barbara, 93106, USA

We present results from a generic search for strongly produced supersymmetric particles in pp collisions in the multijet + missing transverse momentum final state. The data sample corresponds to 2.3 fb^{-1} recorded by the CMS experiment at $\sqrt{s} = 13$ TeV. This search is motivated by supersymmetry (SUSY) models that avoid fine-tuning of the higgs mass. In such models, certain strongly produced SUSY particles, including the gluino and top squark, are predicted to have masses on the order of a TeV. These particles also have some of the highest production cross sections in SUSY and give rise to final states with distinct, high jet multiplicity event signatures. To make the analysis sensitive to a wide range of such final states, events are classified by the number of jets, the scalar sum of the transverse momenta of the jets, the vector sum of the transverse momenta of the jets, and the number of b-tagged jets. No significant excess is observed beyond the standard model (SM) expectation. The results are interpreted as limits on simplified SUSY models. In these models, gluino masses as high as 1600 GeV are excluded at 95% CL for scenarios with low $\tilde{\chi}_1^0$ mass, exceeding the most stringest limits set in by CMS at $\sqrt{s} = 8$ TeV by more than 200 GeV in several simplified models.

1 Introduction

Strongly produced supersymmetric particles, including gluinos and third generation squarks, are among the most attractive search targets in early $\sqrt{s} = 13$ TeV LHC data. At the mass limits set on simplified models [1] with low $\tilde{\chi}_1^0$ mass at $\sqrt{s} = 8$ TeV, the cross section for gluino pair production, for example, is enhanced by a factor of thirty with respect to $\sqrt{s} = 8$ TeV due to the mass-dependent increase in parton luminosity at $\sqrt{s} = 13$ TeV [2]. Consequently, a search for strongly produced SUSY performed at $\sqrt{s} = 13$ TeV needs only a fraction of the data taken at $\sqrt{s} = 8$ TeV to exceed the sensitivity obtained in Run I for many models.

This search is also highly motivated by models of natural SUSY. In these models, the stop, left-handed sbottom, and gluino must have masses near the electroweak scale to compensate for large radiative corrections to the mass of higgs boson from SM particles without fine tuning. Although there is no way to rigorously define what degree of fine tuning is acceptable, a convention among post-Run I natural SUSY models requires the masses of the gluino and top squarks to be less than 2 TeV and 1 TeV, respectively [3,4]. With sufficient data, these models will probed over much of the natural SUSY parameter space in Run II. In R-parity conserving SUSY models, in which the LSP is the $\tilde{\chi}_1^0$, gluinos and squarks are expected to decay to multiple hadrons and weakly-interacting SUSY particles, which escape detection. To target this signature, we conduct our search in a sample of events with multiple jets, large missing transverse momentum (H_T^{miss}), a large scalar sum of jet transverse momenta (H_T), and no charged electrons or muons. Diagrams for three of the simplified SUSY models we target are shown in Figure 1. This analysis [5]

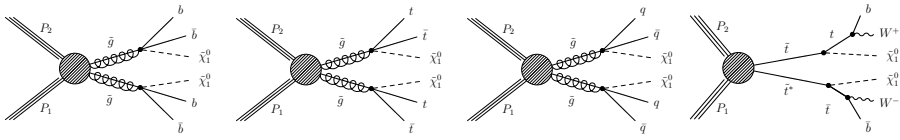

Figure 1 – From left to right, diagrams for the simplified models $pp \to \tilde{g}\tilde{g} \to b\bar{b}b\bar{b}\ \tilde{\chi}_1^0\tilde{\chi}_1^0$, $pp \to \tilde{g}\tilde{g} \to t\bar{t}t\bar{t}\ \tilde{\chi}_1^0\tilde{\chi}_1^0$, $pp \to \tilde{g}\tilde{g} \to q\bar{q}q\bar{q}\ \tilde{\chi}_1^0\tilde{\chi}_1^0$, and $pp \to \tilde{t}\bar{\tilde{t}} \to t\bar{t}\ \tilde{\chi}_1^0\tilde{\chi}_1^0$.

expands and combines strategies from two searches performed by CMS at $\sqrt{s} = 8$ TeV [6,7].

2 Search strategy and event selection

Since SUSY offers an enormous variety of models and final states, we design our search to be inclusive and generic so that we maintain sensitivity to a diverse array of new physics scenarios. We consider events with at least four jets with transverse momenta (p_T) of at least 30 GeV, at least 200 GeV of H_T^{miss}, at least 500 GeV of H_T, and no charged leptons. To increase sensitivity to different signal topologies, and to help characterize a potential excess beyond the measured SM backgrounds, we divide our search region into 72 independent search regions defined by the jet multiplicity, the H_T^{miss}, the H_T, and the b-tagged jet multiplicity of each event. The bins of H_T^{miss} and H_T that define the search regions are illustrated in Figure 2 (left). The dominant SM backgrounds for the all-hadronic multijet + missing momentum final state include production of top quarks and W and Z bosons in association with jets, as well as strongly produced (QCD) multijets. To suppress the multijet background, which arises primarily from mis-measurement of jet momenta, resulting in a fake-H_T^{miss} signature, we reject events in which any of the four jets of largest p_T is aligned with the H_T^{miss}, specifically, we require

$$\Delta\phi(j_i\ ,\ H_T^{\text{miss}}) > 0.5, \quad \Delta\phi(j_j\ ,\ H_T^{\text{miss}}) > 0.3 \tag{1}$$

where $i = 1, 2$ (i.e. the two leading jets) and $j = 3, 4$. Top and W events enter the search region if a W decays either to an electron or muon that is out of kinematic or geometric detector acceptance; if it decays to an electron or muon that fails lepton reconstruction, identification, or isolation requirements; or if it decays to a tau lepton that decays hadronically. To further suppress this background, we reject events with an isolated charged track identified by the particle flow algorithm [8,9] as an electron, muon, or charged hadron.

3 Background estimation

Following the event selection described in Section 2, the dominant background in bins with large jet and b-tagged jet multiplicity is top quark pair production, while in bins with lower multiplicity, the composition is distributed among W, Z, and QCD multijet events. The background composition, as determined in simulation, in select search regions is shown in Figure 2 (center, right).

As the cross sections of these backgrounds are generally larger than those of our target SUSY models by multiple orders of magnitude, many of the search regions with highest signal sensitivity lie on extreme tails of kinematic distributions (Figure 3). The tails of these distributions are difficult to model, so we measure their shapes using dedicated techniques and control regions (CRs) in data for each background process. The CRs are designed to capture the kinematic properties of the backgrounds in the search region up to differences understood sufficiently well that they can be corrected by simulation.

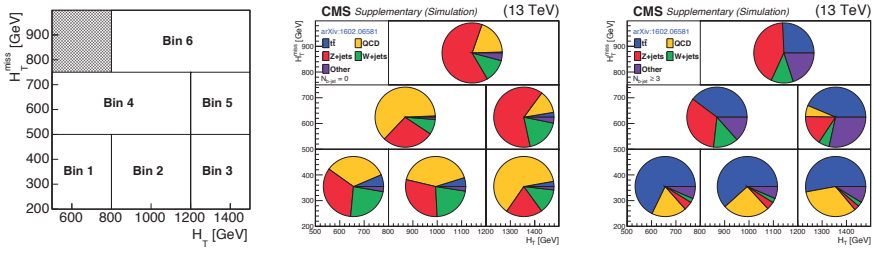

Figure 2 – Search bins in the H_T^{miss} versus H_T plane (left); background composition in the H_T^{miss} versus H_T plane in events with zero b-tagged jets (center); background composition in the H_T^{miss} versus H_T plane in events with three or more b-tagged jets (right). The expected contribution from each process is obtained from simulation after applying the full baseline selection described in Section 2.

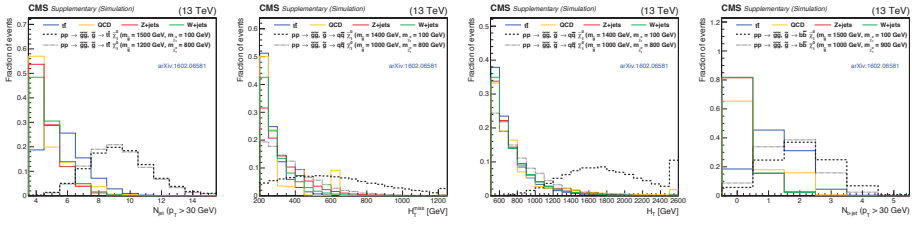

Figure 3 – Distributions from simulated event samples showing kinematic shape comparisons of the number of jets, H_T^{miss}, H_T, and the number of b-tagged jets for the main background processes and six representative gluino production signal models. The full baseline selection is applied in each plot.

4 Results

No significant excess is observed beyond the measured SM backgrounds. Figure 4 shows the observed data are compared to the summed estimated backgrounds in each of the 72 search regions. The results are interpreted as 95% CL upper limits on the production cross sections for simplified SUSY models. Three of these interpretations are shown in Figure 5. The strongest mass limits on gluino pair production are obtained for the model in which the gluino decays exclusively to $\tilde{b}\bar{b}$, yielding the striking final state $b\bar{b}b\bar{b}$ $\tilde{\chi}_1^0\tilde{\chi}_1^0$. For this model, we can exclude gluino masses below 1600 GeV for light $\tilde{\chi}_1^0$ at the 95% CL, an improvement of over 200 GeV with respect to the strongest limits set by CMS at $\sqrt{s} = 8$ TeV. For simplified models in which the gluino decays to $\tilde{t}\bar{t}$ and $\tilde{q}\bar{q}$, we exclude gluino masses below 1550 and 1440 GeV, respectively, for light $\tilde{\chi}_1^0$, also significantly extending previous limits.

References

1. D. Alves *et al*, *J. Phys.* G **10**, 39 (2012).
2. http://www.hep.ph.ic.ac.uk/ wstirlin/plots/plots.html (2013)
3. M. Papucci, J. Ruderman, A. Weiler, CERN-PH-TH (2011)
4. N. Craig, arXiv:1309.0528v2 [hep-ph] (2013)
5. CMS Collaboration, *Phys. Lett.* B **758**, 152180 (2016).
6. CMS Collaboration, *Phys. Lett.* B **725**, 243270 (2013).
7. CMS Collaboration, *JHEP* **06**, 055 (2014).
8. CMS Collaboration, CMS-PAS-PFT-09-001 (2009)
9. CMS Collaboration, CMS-PAS-PFT-10-001 (2010)

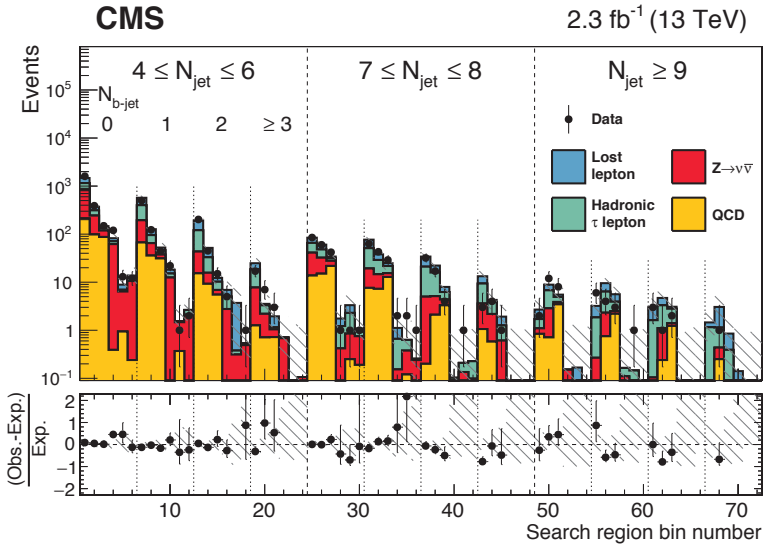

Figure 4 – Observed data and summed data-driven background estimation in each of the 72 search regions

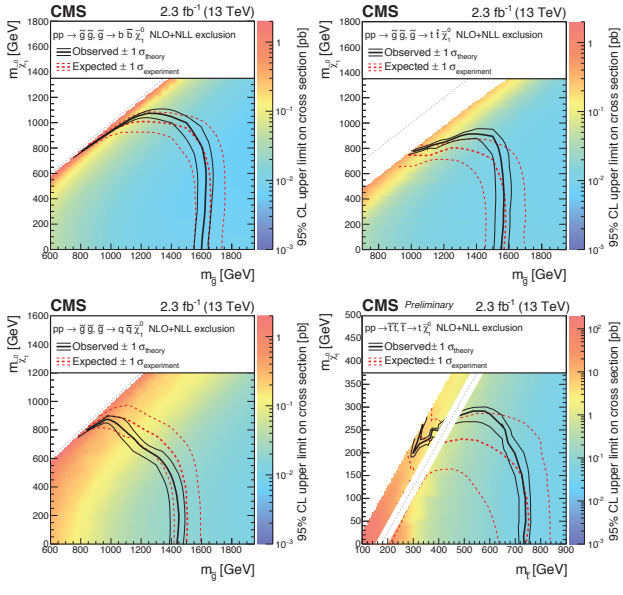

Figure 5 – Clockwise from top-left, 95% CL upper limits on the production cross sections for the simplified models $pp \to \tilde{g}\tilde{g} \to b\bar{b}b\bar{b}\,\tilde{\chi}_1^0\tilde{\chi}_1^0$, $pp \to \tilde{g}\tilde{g} \to t\bar{t}t\bar{t}\,\tilde{\chi}_1^0\tilde{\chi}_1^0$, $pp \to \tilde{t}\bar{\tilde{t}} \to t\bar{t}\,\tilde{\chi}_1^0\tilde{\chi}_1^0$, and $pp \to \tilde{g}\tilde{g} \to q\bar{q}q\bar{q}\,\tilde{\chi}_1^0\tilde{\chi}_1^0$.